16th ICAAR LISBOA 2020-2022

16th International Conference on
Alkali-Aggregate Reaction in Concrete
Lisboa | LNEC | Portugal | 31 May - 2 June 2022

http://icaar2020-2022.lnec.pt

Engineering-based finite element approach to appraise slender and massive ASR-affected structures

R. V. Gorga [(1)], L. F. M. Sanchez [(2)], B. Martín-Pérez [(3)]

(1) University of Ottawa, Ottawa, Canada, rgorg011@uottawa.ca

(2) University of Ottawa, Ottawa, Canada, Leandro.sanchez@uottawa.ca

(3) University of Ottawa, Ottawa, Canada, Beatriz.Martin-Perez@uOttawa.ca

Abstract

Modeling the expansion and damage generated by alkali-silica reaction (ASR) in reinforced concrete structures is very complex, yet necessary to correctly assess the current (diagnosis) and future structural response (prognosis) of distressed concrete members. Several ASR models have been developed over the past decades to predict expansion and damage at different levels, ranging from material (microscopic) to structural (macroscopic) scales. However, those models tend to either neglect or overemphasize the critical physicochemical parameters of the reaction, which limits their applicability. A new simple yet reliable macro-scale finite element (FE) approach is proposed in order to fill this gap. It accounts for the most important parameters affecting ASR through an engineering approach, without the need for non-technical guesses or to "fit" model parameters. The proposed model is validated by simulating both real slender and massive structures, proving its accuracy and applicability.

***Keywords**: finite element; ASR; slender structures; massive structures*

1. INTRODUCTION

Alkali aggregate reaction (AAR) is a complex concrete distress mechanism that results from a chemical reaction between the alkalis from the concrete pore solution and some mineral reactive phases from the aggregates used to make concrete [1]. AAR is normally divided into two different mechanisms, alkali-silica reaction (ASR) and alkali-carbonate reaction (ACR), with ASR being by far the most common. ASR develops when three components are present: aggregate containing reactive mineral phases, high moisture content (normally assumed ≥ 85%), and high alkali content. The reaction produces an expansive gel that may induce tensile stresses, generate cracking, affect the concrete material properties and lead to structural failure. The ASR expansion is highly anisotropic and it is affected by several parameters, including relative humidity, temperature, stress-state, alkali content, aggregate type, aggregate reactivity, etc [2-5].

Esposito [6] classifies the existing ASR models in 4 different categories: micromodels (based on ion diffusion/reaction products), micro-meso-models (based on gel production), meso-models (based on internal pressure) and macro-models (based on concrete expansion). The main goal of the proposed model is to assess the implications of ASR on structural components and (possibly) global systems; therefore, the present work focuses only on macro-models.

The first macro-models used to simulate AAR were very simple due to the limited knowledge and available computational tools at the time, simulating the expansion as an equivalent isotropic expansion [7]. Eventually, the influence of other parameters started being introduced, increasing the accuracy of the simulation. Several approaches were proposed, ranging from continuous-medium models accounting for a relatively small number of parameters [3, 4, 8, 9] to porous-medium models accounting for a very large number of parameters [10].

Even though important progress has been accomplished in the field, there was still need of a model capable of assessing the most important parameters affecting the reaction in a comprehensive and intuitive manner, without overcomplicating (and requiring fitting of parameters) or oversimplifying the description of the reaction and its structural implications. In this context, the engineering-based finite element approach proposed by Gorga et al. [2, 11, 12] was developed.

2. MODEL DESCRIPTION

The model proposed by Gorga et al. [2, 11, 12] uses the concrete damaged plasticity (CDP) model, available in the commercial FE software Abaqus [13], to simulate concrete. This material model describes the elastic and inelastic hydrostatic pressure-dependent behaviour of concrete under both compression and tension [13-15]. Moreover, concrete crushing or tensile cracking are assumed as the main failure mechanisms, with cracking intensity and orientation being evaluated through the development of plastic strain. In summary, if an element or region overcomes the elastic limit, it starts developing plastic strain locally until global equilibrium is reached. This means that, as the load increases, the plastic zone also increases, thus simulating damage accumulation. The mechanical properties deterioration (i.e., reduction of modulus of elasticity, compressive strength and tensile strength) is assumed to be a function of the AAR expansion level, according to Sanchez et al. [16].

AAR expansion is modeled by imposed an anisotropic and stress-state dependent equivalent AAR strain, according to Gautam et al. [5], which is implemented through an Abaqus user subroutine (USDFLD). The unrestrained reaction kinetics and expansion prediction over time (i.e., reference free expansion input curve) are calculated according to the physicochemical analytical model developed by Goshayeshi [17]. As described by Gorga et al. [11], the analytical AAR model is able to roughly capture the in-service expansion potential based on results reported by [18] and [19].

Steel is modelled as an elasto-plastic material for both rebars and prestressing strands, following the real stress-strain curve of the material. Prestressing is imposed as equivalent negative thermal gradient.

When necessary, thermo-mechanical structural behaviour over time is modelled by describing all materials as linear-elastic and imposing both thermal and mechanical boundary conditions (displacement, convection, radiation and heat generation). Stresses are checked to verify the applicability of the approach (no concrete cracking or crushing and no steel yielding). If the assumption is valid, the residual thermal stresses from the transient thermo-mechanical analyses can then be used as initial boundary condition on the non-linear mechanical ASR model.

The authors performed a total of four validations before using the proposed approach to simulate real structures, including simulating sound reinforced concrete, sound prestressed concrete, thermal behaviour of sound concrete and ASR-affected reinforced concrete. All validations were based on experimental results obtained through laboratory tests.

As shown in Figure 2.1, modelling sound reinforced and prestressed concrete proved that the material models and modeling approach was able to accurately represent the structural behaviour of the reinforced concrete members up to (shear or bending) failure. Experimental values were obtained from [20] for reinforced concrete and [21] for prestressed concrete.

Modeling the thermal behaviour of sound concrete proved that the proposed approach is able to accurately simulate concrete's heat of hydration and temperature stabilization over time (Figure 2.2). Experimental values used were from a 1 m³ mass concrete cube cast and stored in a lab [22].

Lastly, the anisotropic stress-state dependent ASR expansion behaviour [5] was validated by simulating ASR-affected push-off specimens with different amounts of reinforcement confinement [19] (Figure 2.3). Even though results for the four stirrups (4S) were slightly higher than the experimental values for several reasons, results were found to be accurate overall.

3. ASR-AFFECTED SLENDER STRUCTURE – ROBERT-BOURASSA CHAREST OVERPASS

3.1 Overall structure and model description

Robert-Bourassa Charest (RBC) overpass was an ASR-affected highway bridge structure built in 1966 in Quebec City, Canada. The reinforced concrete structure comprised a deck of varying thickness, four rows of eight Y-shaped piers and massive concrete foundations [23]. The piers were classified in 2 different categories: exposed (E) and non-exposed (NE) piers [24]. Exposed piers were assumed to be highly subjected to solar radiation, weathering (rain, snow, freezing rain, etc.), pollution and splashing of both water and de-icing salts. Conversely, non-exposed piers were considered to be mostly protected from those factors because of their surroundings. The overall geometry of the RBC is shown in Figure 3.1.

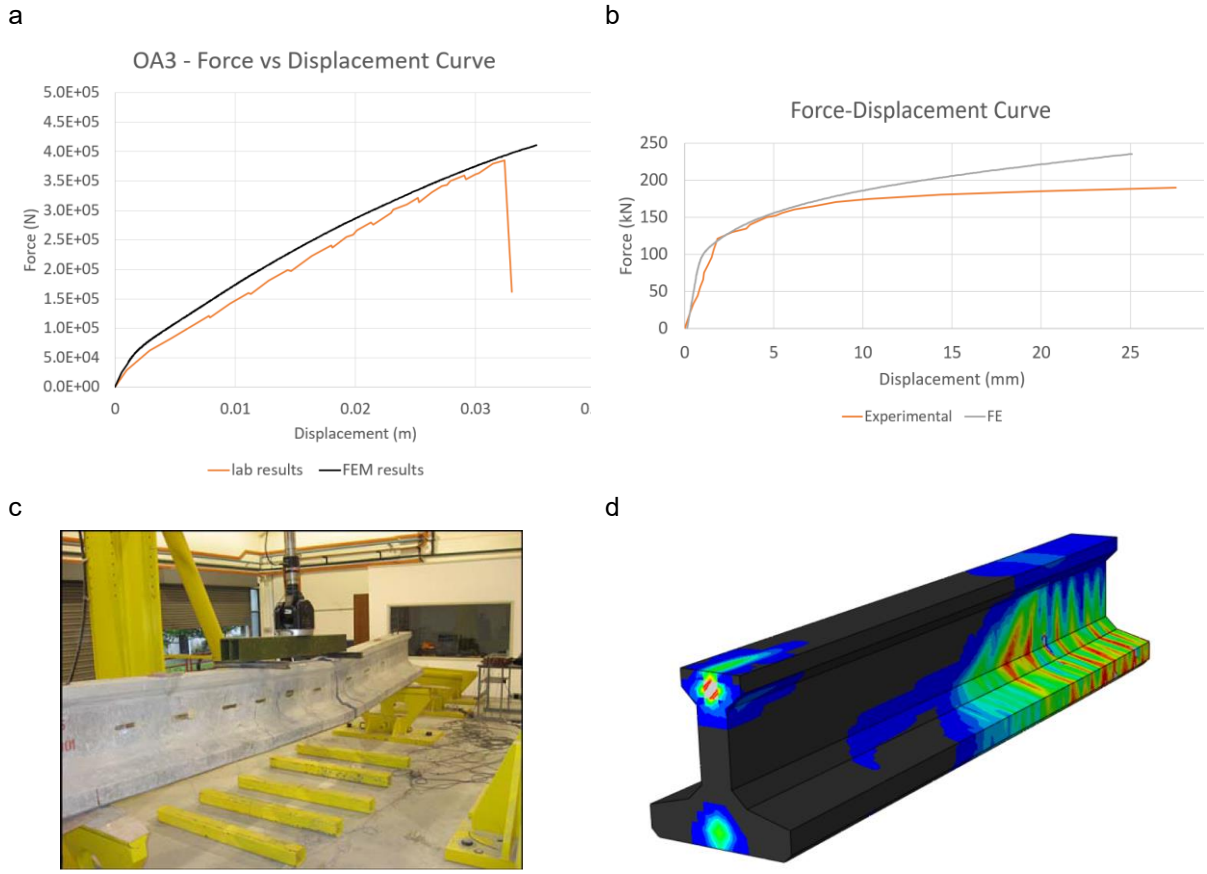

Fig. 2.1: Sound concrete validations: a. Reinforced concrete experimental and FE force-displacement curves [2], b. Prestressed concrete experimental and FE force-displacement curves [11], c. Prestressed concrete cracking pattern recorded in the lab [21], d. Prestressed concrete cracking pattern (plastic strain) predicted by the FE model for half the beam [11].

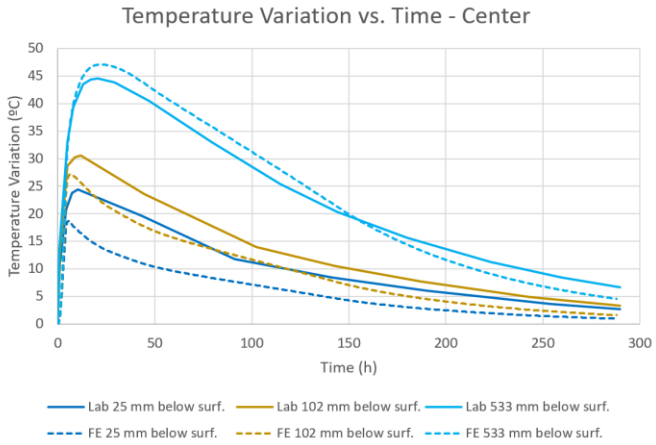

Figure 2.2: Temperature variation vs. time at the center of concrete block. Source: [12]

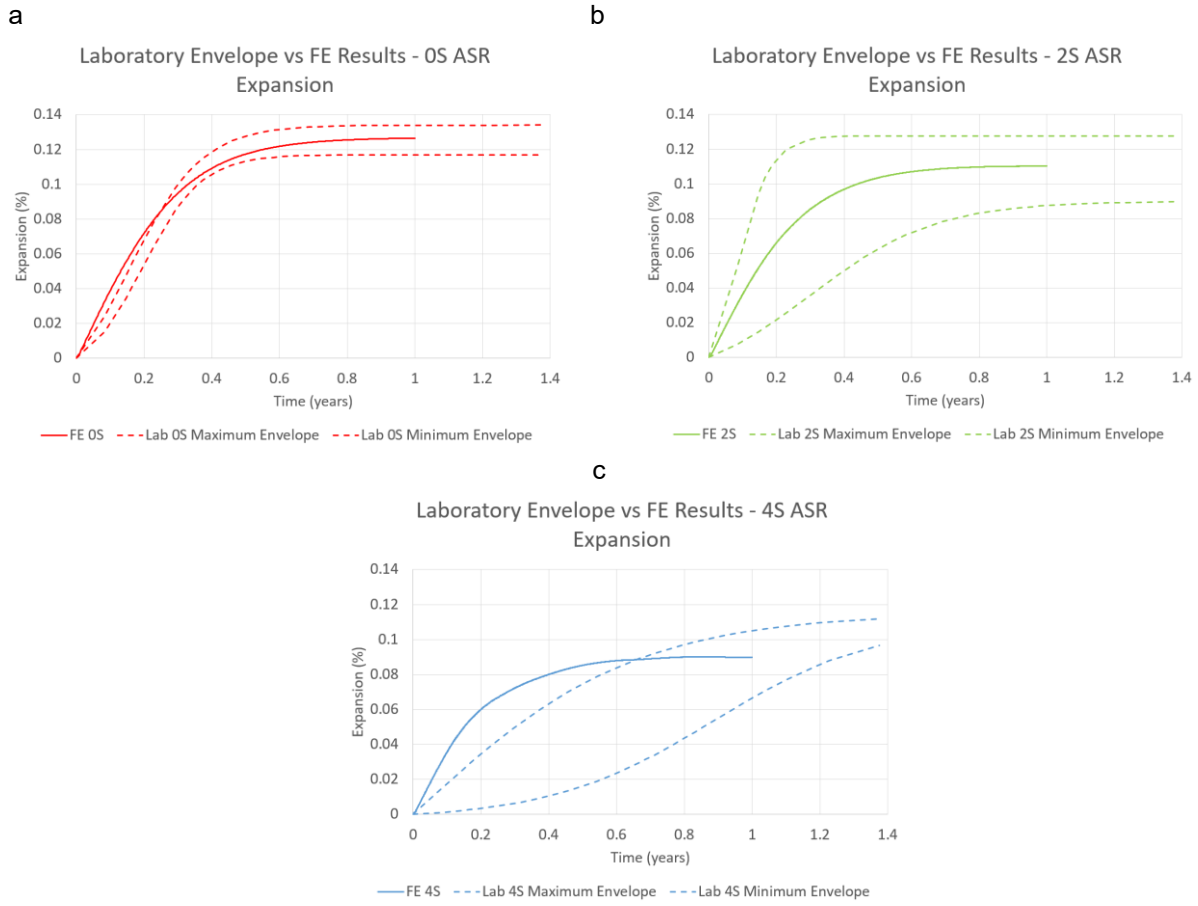

Figure 2.3: Expansion vs time curve - FE results and lab envelopes [2]: a. 0S (no stirrups), b. 2S (two stirrups), c. 4S (four stirrups)

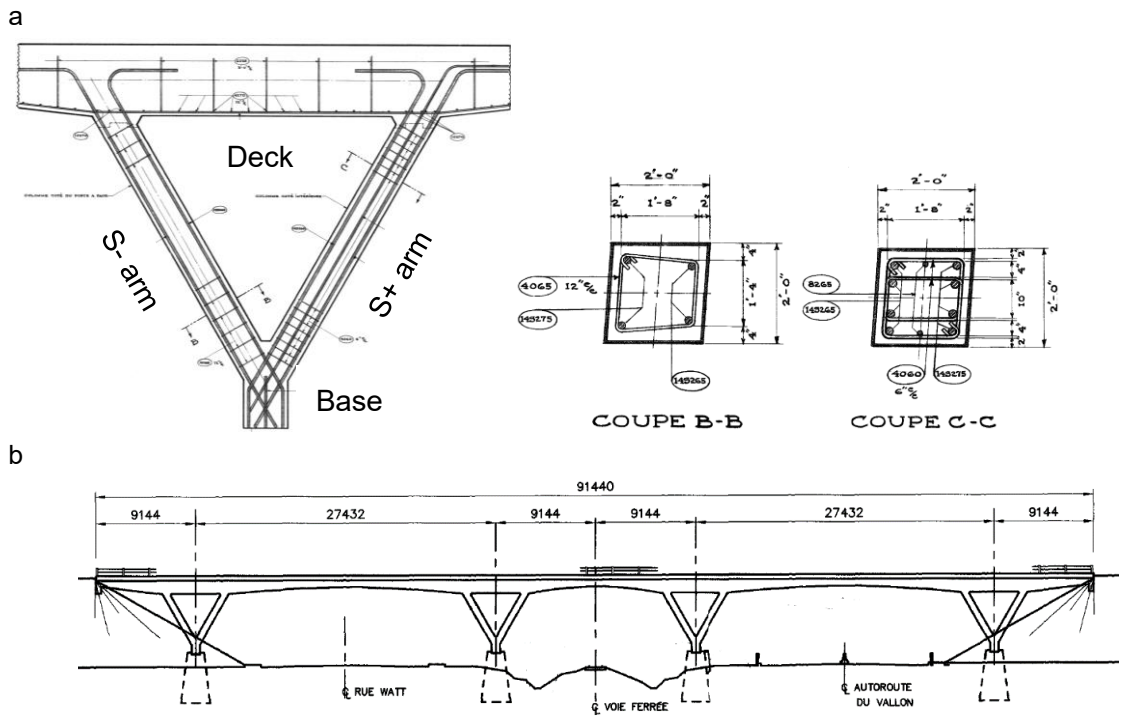

Figure 3.1: Y-shaped pier original design: a. Reinforcement detail (dimensions in inches), b. Overpass longitudinal view (dimensions in mm). Source: Adapted from [25].

Over the last three decades, several distress signs were observed on various structural members [26]. The deck presented steel corrosion and concrete delamination/spalling. The foundation showed signs of concrete map cracking, scaling, disaggregation and pop-outs. The piers presented concrete spalling and steel corrosion. According to microscopic analyses, the prior distress signs were mainly triggered by ASR and freeze-thaw (FT) cycles. Due to the extent of damage and results from laboratory tests, the structure was considered unsafe and was demolished in 2010/2011. However, prior to the demolition, cores were extracted and some pier arms were taken to a laboratory for further microscopic and mechanical (macroscopic) analyses [27]. The data from these tests enabled a thorough evaluation of the bridge's damage degree at the time of the demolition.

Amongst the analyses performed, interesting results were obtained through the Damage Rating Index (DRI), a microscopic tool often used to appraise damage and development of internal swelling reaction (ISR) mechanisms such as AAR [27]. Results were able to determine an equivalent expansion level for each exposure class, which can be understood as the estimated ASR development (or expansion attained to date) needed to cause a damage degree similar to that observed in the DRI procedure. An average value of 0.05% for the NE piers and between 0.09% for the E piers was determined, even though the aggregate was considered highly reactive and would present a free expansion potential of 0.20-0.25% in the concrete prism test according to CSA [28].

Moreover, strain relief tests were performed on the stirrups of both piers [27]. The strain was measured using strain-gauges at the middle of stirrups of the S+ arm. Average values indicated that the average strain was equal to 569 μstrain for the NE piers and 1290 μstrain for the E piers.

A model of the pier was created for each exposure condition, accounting for the local climatic data, reinforcement confinement [29], concrete creep and mechanical properties deterioration as a function of the expansion level (Table 3.1) [11]. It was assumed that the temperature of the entire slender member is the same, but the relative humidity of the environment was assumed to only affect the concrete cover, with the core being saturated (based on the equations proposed by [4] and [30]. The influence of all additional phenomena affecting the exposed pier (e.g., sun radiation and its consequent hourly variations of temperature or temperature gradients, exposure to rain and snow, exposure to de-icing salts, splashing due to traffic, pollution, etc.) was accounted for indirectly by changing the reference temperature and relative humidity. The temperature was increased by 13.5ºC according to the temperature differentials for exposure conditions of concrete structures (summer conditions) from CSA [31]. Three approaches to alter the reference relative humidity were assessed: using the original values, assuming global increase and assuming local (cover only) increase. The new relative humidity was calculated by assuming 100% RH whenever it rained and the following day, based on the local daily values of precipitation.

Table 3.1: Mechanical properties deterioration. Source: [16]

Expansion [%]	0.05%	0.12%	0.20%
f'_c reduction [%]	6.8	0.6	11.0
E reduction [%]	9.1	36.3	44.8
f'_t reduction [%]	6.5	62.0	78.8

3.2 Discussion of results

Analyses indicated that the best approach to simulate the effect of exposure is to increase the temperature and use the original relative humidity values, which is the only value discussed hereafter [11].

The predicted equivalent damage, based on microscopic analyses, matched well the reference expansion curves yielded by the analytical ASR model when the climatic conditions were considered, as shown in Table 3.2.

Similarly, the stirrup strain obtained from the finite element model also matched the values measured in the laboratory [11]. An error of 3.2% was observed for the non-exposed case and -32.6% for the exposed case. This means that the proposed model is capable of accurately simulating the effects of the reaction when the climatic conditions are accounted for and the member is protected. Moreover, the authors explain that the underestimation of the strain value for the exposed case is likely because the effect of freeze-thaw (FT) cycles was not simulated. Microscopic analyses estimated that approximately 25% of

the damage observed on the exposed pier was due to FT; therefore, corroborating the assumption that ASR was modeled correctly.

Table 3.2: Equivalent (measured) vs reference (analytical) expansions. Source: [11].

Case	Equivalent Expansion [%]	Reference Expansion [%]	
Non-Exposed	0.05	NE core	0.06
		NE cover	0.04
Exposed	0.09	E core (RH original)	0.11
		E cover (RH original)	0.07

The cracking pattern obtained by the model matched the cracking orientation, cracking intensity and location of spalling/delamination observed in the field for both cases, as shown below. Note that regions in blue are lightly damaged, regions in red are moderately damaged and regions in light grey are highly damaged (largest cracks and/or indication of possible spalling or delamination).

a b

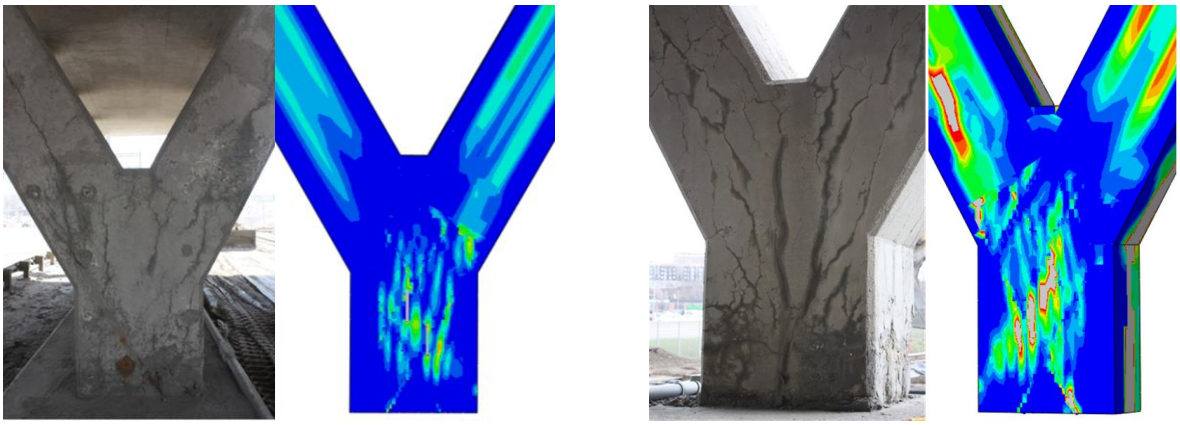

Figure 3.2: Damage on the base of the pier (real and FE model plastic strain) at time of demolition: a. Non-exposed case, b. Exposed case. Source: [11].

Lastly, it was observed that the structure was near global failure at the time of demolition, given that several stirrups in the exposed pier had already yielded due to ASR expansion. Therefore, the model results support the decision to demolish the overpass. The reinforcement stresses are shown below.

a b

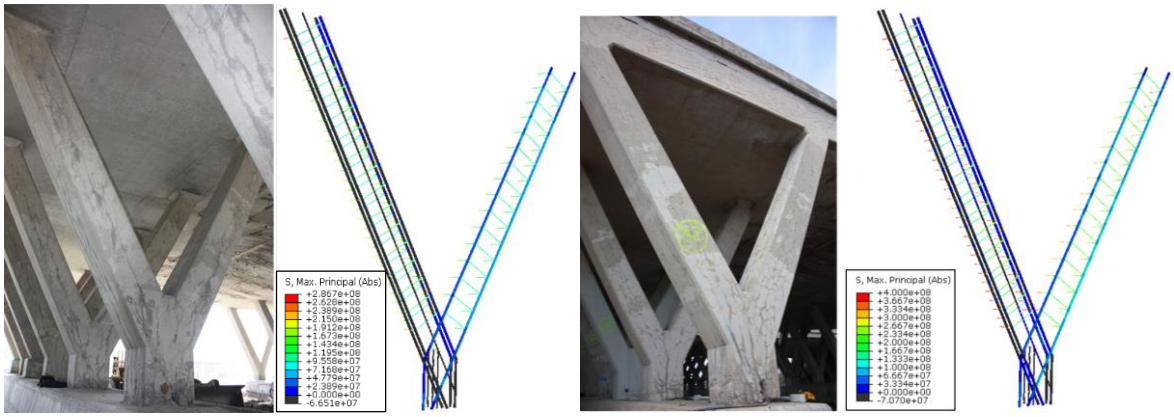

Figure 3.3: Observed damage on the pier and FE model stress on reinforcement at time of demolition: a. Non-exposed case, b. Exposed case. Source: [11].

4. ASR-AFFECTED MASSIVE STRUCTURE – PAULO AFONSO IV DAM

4.1 Overall structure and model description

The chosen structure for this analysis was Paulo Afonso IV (PAIV) dam spillway, shown in Figure 4.1. The dam is located in the city of Paulo Afonso, PE, Brazil, and it is owned by the Companhia Hidro-Elétrica do São Francisco (CHESF), who provided the data presented hereafter [12]. The dam was built between 1975 and 1981, with the first signs of ASR being observed in 1985. Even though several distress signs have been observed on the dam, its performance has not been completely compromised and it is currently still in operation. The most commonly observed distress signs are map cracking, alkali-silica gel leaching and water leaking.

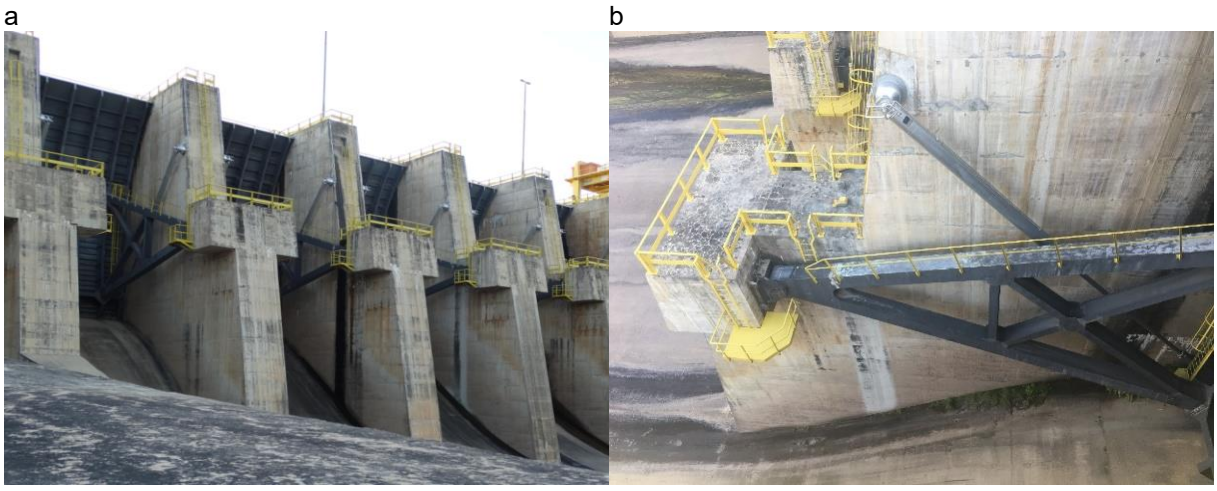

Fig. 4.1. Paulo Afonso IV dam - Spillway: a. Overview, b. Close-up of the ASR damage.

Standard laboratory tests were performed to determine the material properties of the concrete [32] and DRI tests were performed to determine the equivalent expansion level of the structure. Additionally, expansion measurements from extensometers were also obtained directly from CHESF.

The analysis of the dam was divided in two parts [12]. First, a linear-elastic thermo-mechanical analysis of the spillway was performed to determine the stress-state due to thermal loads, as well as the variation of the temperature profile of the dam. Then, the residual thermal stresses were imported into a non-linear mechanical ASR model, which included both the long-term loads, the residual thermal stresses and the reaction's expansion.

For both analyses, creep and prestressing steel relaxation were accounted for and the reference mechanical properties of the concrete were determined based on laboratory tests [32]. The material properties of the linear-elastic thermo-mechanical analysis assumed no deterioration (based on the premise that ASR would not have had time to develop yet), while the mechanical properties of the non-linear mechanical ASR analysis were assumed to vary over time as a function of the expansion [16].

Soil was modeled through spring elements and hydrostatic loads were applied both directly on the structure and as pressure/surface traction load on the beam due to the water load on the gate. The heat of hydration was modelled as heat generation per mass energy per mass based on [22], who described the heat generated over time for a similar mass concrete mix. Different reference (input) ASR expansions [17]were imposed for each of the six isothermal regions. The entire spillway was assumed to be fully saturated, because the environmental relative humidity only affects the first few outer centimeters of the structure [30] and the dimensions of the finite elements was between 25 and 50 cm. Moreover, massive structures are known to present almost no leaching due to their size in comparison to slender structures and concrete cores [33]. The AAR analytical model [17] was based on concrete cores, which presented significant leaching; therefore, the amount of alkalis was increased to simulate the effect of the lack of leaching. In general, ASR-affected concrete cores lose between 3 and 20% of alkalis in the first 4 weeks and between 10 and 50% after one year (duration of the test) [33]. Therefore, the alkali content for the entire structure was conservatively increased by 50%, given that this phenomenon is only being accounted for indirectly.

4.2 Discussion of results

Results from the linear-elastic thermo-mechanical analysis indicated that temperature alone was not enough to generate (macro) cracking or crushing; therefore, assuming this analysis as linear-elastic was deemed acceptable [12]. Thermal micro-cracking was assumed to be negligible. Moreover, it was also found that the heat of hydration would not significantly affect the reaction as the internal dam temperature would stabilize in less than two years.

A total of five free expansion curves (Figure 4.2) were compared to the equivalent expansion level from the DRI test. Those included the analytical AAR model [17], analytical AAR model with average measured rate, analytical AAR model with maximum measured rate, constant average rate expansion and constant maximum rate expansion. Note that some authors [34] defend the hypothesis that ASR-induced expansion in massive structures can either continue indefinitely and/or be assumed as linear. In general, this phenomenon is assumed to be due to the alkali release from aggregates, additional source of reactive silica minerals from large aggregates and the absence (or very little amount) of leaching [12].

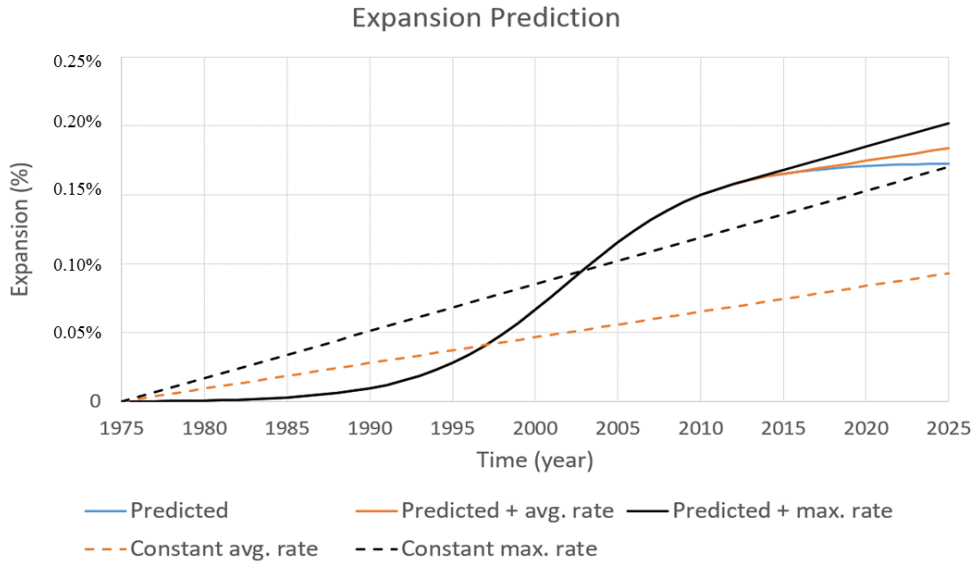

Fig. 4.2. Representative AAR expansion curves

The DRI tests done by CHESF (according to [35]) were converted to the new approach proposed by [36], which is more reliable and accurate to assess ASR-induced expansion and damage [37]. Even though significant scattering was observed due to the intrinsic anisotropic nature of ASR, small number of extracted cores evaluated by CHESF and, conversion of the DRI values, results indicated that the equivalent expansion level for the spillway would be between moderate and high reactivity (between 0.12 and 0.20%) [12]. All analytical AAR curves predict that the expansion would be around 0.13% in 2007 (year of DRI test), indicating that the assumptions previously described seem to be correct and likely can indirectly be used to simulate the effects of AAR on massive structures. Conversely, both constant rate (linear) curves underestimate the expansion predicted by the laboratory test (0.06% and 0.11% in 2007, respectively). Note that the aggregate used in PAIV is considered to be a moderately reactive aggregate (i.e., ± 0.12% at one year according to the concrete prism test - CPT).

It is also interesting to note that the model predicted cracking initiation would happen only in 1991, whereas CHESF reported that the first major crack due to ASR was observed in 1985 [12]. Therefore, if the curves based on the analytical model were shifted by 6 years, the damage that would have been achieved in 2007 (0.16%) would be much closer to the expansion predicted through the DRI (0.12-0.20%). Hence, there is a strong indication that the previously described phenomena affecting the reaction in massive structures (i.e., alkalis release from aggregates, absence/little amount of alkalis leaching, etc.) may significantly affect the initial kinetics and expansion over time.

A comparison between the resulting FE cracking pattern and the observed damage for the year 2018, based on the predicted expansion curve (solid blue line), is presented next.

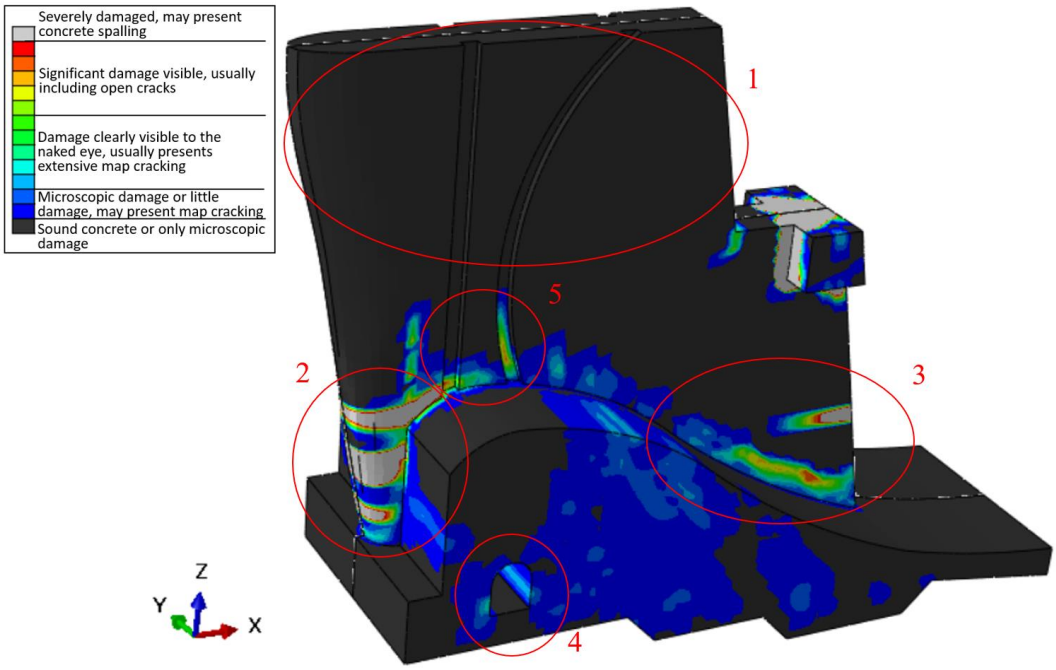

Fig. 4.3. PA-IV FE predicted damage with emphasis on 5 different regions: 1) Top of the column, 2) Upstream base of the column, 3) Downstream base of the column, 4) Gallery and 5) Main radial gate and emergency gate. Source: [12].

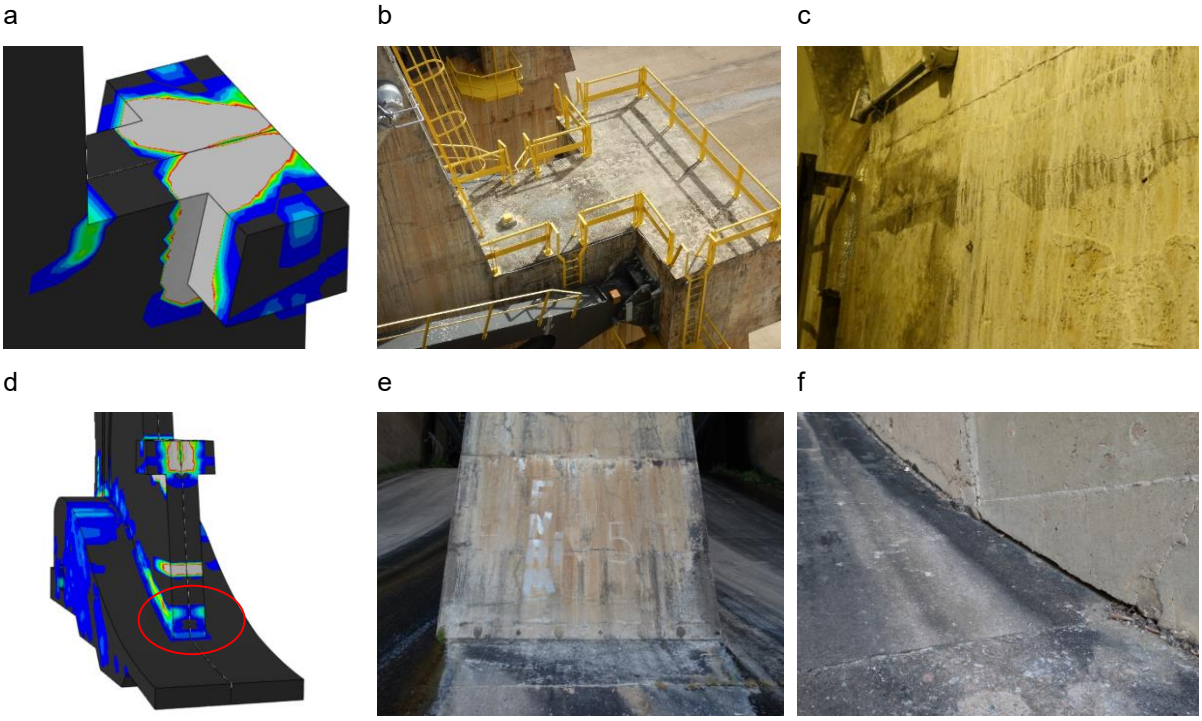

Fig. 4.4. PA-IV: a. FE predicted damage on beam, b. Observed damage on beam, c. Observed damage on gallery, d. FE predicted damage on the back of the column's base (downstream), e. Observed damage on the back of the column's base (downstream), f. Observed damage on the side of the column's base (downstream). Source: [12].

Several conclusions can be drawn from the presented figures [12]. First, the damage at the top of the beam was clearly captured (Figure 4.4 a and b). Long-term loads generated a small amount of cracking, but the damage significantly increased due to ASR in this critical region.

Second, the model did not predict damage at the top of the column (Figure 4.3 region 1), even though damage was observed there (Figure 4.1 b). This happened because the the interface between concrete layers (discontinuity) was not modeled and because the top of the column was unrestrained (5mm gate gap on Y direction). The authors observed that the displacement would be equal to 2.16mm in 2018 and that the displacement allowance (5mm) would likely not be reached during the service life of the structure, which means that the gate operation should not be affected by ASR expansion.

The model also predicted significant damage on the upstream face of the column (Figure 4.3 region 2). Unfortunately, it was not possible to verify the condition of that region as it was submerged in water.

The observed damage on the wall of the gallery (Figure 4.4 c), on the back of the column's base (Figure 4.4 e) and on the side of the column's base (Figure 4.4 f) were all correctly captured by the model (Figure 4.3 region 4, Figure 4.3 region 3 and Figure 4.4 e, respectively).

Lastly, the authors observed that the model predicted a large crack behind the radial gate (Figure 4.3 region 5) and that it was locally affecting the prestressing tendons. In 2018 the maximum tendon stress is equal to 1570 MPa, very close to the yielding stress (1580 MPa) and not too far away from the ultimate stress of the prestressing strands (1860 MPa). It was not possible to verify if the predicted crack actually exists due to the difficult access to the region. Even so, it is highly recommended that this region be monitored to avoid possible problems in the near future.

5. ONGOING RESEARCH

Even though significant progress has been accomplished through the validations and analyses previously described, more work is still necessary to further improve the proposed approach. In this context, another two research topics are currently under development. First, the model will be used to simulate the highly distressed Champlain Bridge, in Montreal, Canada. Corrosion will be incorporated into the model to assess the impact of the combined action of both distress mechanisms. Second, the structural implications of slot-cutting on ASR-affected dams is being evaluated, with special emphasis being given to creep effects.

6. CONCLUSION

AAR expansion is a complex and anisotropic phenomenon, affected by several parameters. Even though several modelling approaches exist to assess AAR-affected structures, the one proposed by Gorga et al. [2, 11, 12]) deserves special attention for being able to accurately simulate both slender and massive AAR-affected structures without fitting parameters to match observed data. There is still plenty of room for improvement, as presented when discussing the ongoing research, but it's accuracy and easy applicability make it an attractive alternative to simulate AAR both academically and in the private sector.

7. REFERENCES

[1] Fournier B, Bérubé A (2000) Alkali-aggregate reaction in concrete: a review of basic concepts and engineering implications. Canadian Journal of Civil Engineering 27(2):167–91. https://doi.org/10.1139/cjce-27-2-167

[2] Gorga RV (2018) Engineering-Based FE Approach to Appraise Slender Structures Affected by Alkali-Aggregate Reaction (AAR). Ottawa, ON, Canada: MASc Thesis - University of Ottawa.

[3] Saouma V, Perotti L (2006) Constitutive model for alkali-aggregate reactions. ACI Materials Journal 103: 194–202. https://doi.org/10.14359/15853

[4] Ulm F, Coussy O, Li K, Larive C (2000) Thermo-chemo-mechanics of ASR expansion in concrete structures. ASCE Journal of Engineering Mechanics, 126:233–242. https://doi.org/10.1061/(ASCE)0733-9399(2000)126:3(233)

[5] Gautam BP, Panesar DK, Sheikh SA, Vecchio FJ (2017) Multiaxial expansion-stress relationship for alkali silica reaction-affected concrete. 114(1). https://doi.org/10.14359/51689490

[6] Esposito R, Hendrix M A N (2012) Degradation of the mechanical properties in ASR-affected concrete: Overview and modeling. Aix-en-Provence, France, Strategies for Sustainable Concrete Structures - Numerical Modeling.

[7] Charlwood R (1994) A review of alkali aggregate in hydro-electric plants and dams. International Journal on Hydropower Dams, 73–80.

[8] Pan J, Feng Y, Xu Y, Jin F (2013) Chemo-damage modeling and cracking analysis of AAR-affected concrete dams. Science China – Technological Sciences, 56(6):1449-1457. https://doi.org/10.1007/s11431-013-5187

[9] Winnicki A, Serega S, Norys F (2014) Chemoplastic modelling of alkali-silica reaction (ASR). Computational Modelling of Concrete Structures (EURO-C), 2:765–774. https://doi.org/10.1201/b16645-86

[10] Grimal E, Sellier A, Le Pape Y, Bourdarot E (2008) Creep, shrinkage, and anisotropic damage in alkali-aggregate reaction swelling mechanism-Part I: A constitutive model. ACI Materials Journal, 105:227–235. https://doi.org/10.14359/19818

[11] Gorga RV, Sanchez LFM, Martin-Perez B (2018) FE approach to perform the condition assessment of a concrete overpass damaged by ASR after 50 years in service. Engineering Structures. 177:133-146. https://doi.org/10.1016/j.engstruct.2018.09.043

[12] Gorga RV, Sanchez LFM, Martin-Perez B, Fecteau PL, Cavalcanti A, Silva P (2020) Finite Element Assessment of the ASR-Affected Paulo Afonso IV Dam. Journal of Performance of Constructed Facilities. 34(4). https://doi.org/10.1061/(ASCE)CF.1943-5509.0001456

[13] Simulia DSC (2014). Abaqus/CAE - Complete Abaqus Environment - version 6.14, Providence, RI, USA: Simulia Dassault Systèmes Corporation.

[14] Bompa DV, Onet T (2010) Identification of concrete damaged plasticity constitutive parameters. The National Technical Scientific Conference – Modern Technologies for the 3rd Millenium. Oradea, Romenia.

[15] Wahalathantri BL, Thambiratnam DP, Chan THT, Fawzia S (2011) A material model for flexural cracks simulation in reinforced concrete elements using ABAQUS. Brisbane, Australia: eddBE2011. 260-264.

[16] Sanchez LFM, Fournier B, Jolin M, Mitchell D, Bastien J (2017) Overall assessment of Alkali-Aggregate Reaction (AAR) in concretes presenting different strengths and incorporating a wide range of reactive aggregate types and natures. Cement and concrete research, 93:17-31. https://doi.org/10.1016/j.cemconres.2016.12.001

[17] Goshayeshi N. (2019) Contribution to the development of analytical models to forecast ankali-aggregate reaction (AAR) kinetics and induced expansion. Ottawa, ON, Canada: MASc Thesis - University of Ottawa.

[18] Fournier B, Chevrier R, Bilodeau A, Nkinamubanzi PC, Bouzoubaa N (2016) Comparative field and laboratory investigations on the use of supplementary cementing materials (SCM) to control alkali-silica reaction (ASR) in concrete. 15th International Conference on Alkali-Aggregate Reaction - ICAAR, São Paulo, Brazil.

[19] Sanchez LFM, Fournier B, Bastien J, Mitchell D (2016) Assessment of structures subjected to concrete degradation. ASCET, Quebec, Canada.

[20] Vecchio FJ, Shim W (2004) Experimental and analytical reexamination of classic concrete beam tests. 130(3):460-469. https://doi.org/10.1061/(ASCE)0733-9445(2004)130:3(460)

[21] Cheng HT, Mohammed BS, Mustapha KN (2015) Experimental and analytical analysis of pretensioned inverted T-beam with circular web openings. International Journal of Mechanics and Materials in Design 5:203-215. https://doi.org/10.1007/s10999-009-9096-4

[22] Lawrence AM (2009) A finite element model for the prediction of thermal stresses in mass concrete. Gainesville, U.S.A.: Ph.D. Thesis - University of Florida.

[23] ICAAR Visit Report (2000) Report of the visit of structures affected by AAR in the Quebec City area. 11th ICAAR - International conference on alkali-aggregate reaction, Quebec, Canada.

[24] Sanchez LFM, Noel M, Santos VAA (2018) Techniques to Rehabilitate Bridge Columns Affected by Alkali-Silica Reaction (ASR). 9th International Conference on Bridge Maintenance, Safety and Management - IABMAS, Melbourne, Australia. https://doi.org/10.1201/9781315189390-145

[25] M.o.T.o.Q. MTQ (1964) Report on the Robert-Bourassa Charest overpass reinforcement and overall dimensions. Internal communication, Quebec City, Canada.

[26] Bérubé M, Smaoui N, Fournier B, Bissonnette B, Durand B (2005) Evaluation of the expansion attained to date by concrete affected by ASR - Part III: Application to existing structures. Canadian Journal of Civil Engineering, 32:463-479. https://doi.org/10.1139/l04-104

[27] Sanchez LFM, Fournier B, Bastien J, Mitchell D, Noël M (2016) Overall assessment of an ASR affected overpass "Robert-Bourassa/Charest" after nearly 50 years in service. Foz do Iguaçu, Brazil. https://doi.org/10.1201/9781315207681-278

[28] CSA A23.2-14A (2014) Potential Expansivity of Aggregates; Procedure for Length Change Due to Alkali-Aggregate Reaction in Concrete Prisms. Canadian Standards Association, Missisauga, Ontario, Canada.

[29] Saatcioglu M, Razvi SR (1992) Strength and ductility of confined concrete. ASCE Journal of Structural Engineering, 118(6):1590-1607. https://doi.org/10.1061/(ASCE)0733-9445(1992)118:6(1590)

[30] Comi C, Kirchmayr B, Pignatelli R (2012) Two-phase damage modeling of concrete affected by alkali–silica reaction under variable temperature and humidity conditions. International Journal of Solids and Structures, 49(23,24):3367–3380. https://doi.org/10.1016/j.ijsolstr.2012.07.015

[31] CSA S6-14 (2014) Canadian highway bridge design code. Canadian Standard Association, Missisauga, Ontario, Canada.

[32] Cavalcanti AJCT, Juliani MAC, Becocci L, Carrazedo R (2006) Avaliação dos Efeitos da Reação Álkali-Agregado no Vertedouro da Usina de Paulo Afonso IV. II Simpósio sobre Reação Álkali-Agregado em Estruturas de Concreto - RAA 2006 – IBRACOM, Rio de Janeiro, Brazil.

[33] Lindgård AJ, Thomas MDA, Sellevold EJ, Pedersen B, Andiç-Çakır Ö, Justnes H, Rønning TF (2013) Alkali-silica reaction (ASR)-performance testing: influence of specimen pre-treatment, exposure conditions and prism size on alkali leaching and prism expansion. Cement and Concrete Research, 53: 68–90. https://doi.org/10.1016/j.cemconres.2013.05.020

[34] Gocevski V, Yildiz E (2017) Macro-modelling of AAR-affected hydraulic structures. Chambéry, France, Wiley.

[35] Grattan-Bellew P, Danay A (1992) Comparison of laboratory and field evaluation of AAR in large dams. International Conference on Concrete AAR in Hydroeletric Plants and Dams. Frederickton, Canada: Canadian Electrical Association & Canadian National Committee of the International Commission on Large Dams, 23.

[36] Villeneuve V, Fournier B (2012) Determination of the damage in concrete affected by ASR – the damage rating index (DRI). 14th ICAAR - International Conference on Alkali-Aggregate Reaction in Concrete, Austin, Texas, U.S.A.

[37] Sanchez LFM Fournier B, Jolin M, Duchesne J (2015) Reliable quantification of AAR damage through assessment of the damage rating index (DRI). Cement and Concrete Research, 67: 74-92. https://doi.org/10.1016/j.cemconres.2014.08.002